Imaginary time correlations and the phaseless auxiliary field quantum Monte Carlo

M. Motta, D. E. Galli, S. Moroni, and E. Vitali

Citation: The Journal of Chemical Physics **140**, 024107 (2014); doi: 10.1063/1.4861227
View online: http://dx.doi.org/10.1063/1.4861227
View Table of Contents: http://scitation.aip.org/content/aip/journal/jcp/140/2?ver=pdfcov
Published by the AIP Publishing

Imaginary time correlations and the phaseless auxiliary field quantum Monte Carlo

M. Motta,[1] D. E. Galli,[1] S. Moroni,[2] and E. Vitali[1]
[1]*Dipartimento di Fisica, Università degli Studi di Milano, via Celoria 16, 20133 Milano, Italy*
[2]*IOM-CNR DEMOCRITOS National Simulation Center and SISSA, via Bonomea 265, 34136 Trieste, Italy*

(Received 21 October 2013; accepted 23 December 2013; published online 13 January 2014)

The phaseless Auxiliary Field Quantum Monte Carlo (AFQMC) method provides a well established approximation scheme for accurate calculations of ground state energies of many-fermions systems. Here we address the possibility of calculating imaginary time correlation functions with the phaseless AFQMC. We give a detailed description of the technique and test the quality of the results for static properties and imaginary time correlation functions against exact values for small systems. © *2014 AIP Publishing LLC*. [http://dx.doi.org/10.1063/1.4861227]

I. INTRODUCTION

Over the last decades the study of many body quantum systems at zero temperature has been systematically supported by *ab initio* Quantum Monte Carlo (QMC) calculations. QMC are methods relying on a stochastic solution of the imaginary time Schrödinger equation of the system. As far as *bosonic* degrees of freedom are considered, QMC calculations allow static properties, energetics, and structure functions, to be computed *exactly*[1–6] even for strongly correlated systems, for which analytic approaches yield only approximate results. Furthermore, the possibility of reconstructing dynamical properties of bosonic systems, like excitation spectra and response functions, from imaginary time correlation functions (ITCFs) has been explored with remarkable results.[3,7–13] On the other hand, for fermionic degrees of freedom the situation is considerably complicated by the well-known *sign problem*:[14,15] the computational cost increases exponentially with the system size. The most widely employed scheme to reduce the problem to polynomial complexity is the *Fixed-Node* (FN) approximation:[16,17] FN restricts the stochastic sampling of the *configurational space* to regions where the sign of a reasonable approximation for the ground state wave function, the *trial wave function*, remains constant. Such approximation provides very accurate estimations of ground state properties.[16–19] Nevertheless, FN may give inaccurate results for imaginary time correlation functions even when the nodal structure of the ground state wave function is exactly known: as an example, in Fig. 1 we show the comparison between exact and FN imaginary time correlation functions of the density fluctuations $\langle \hat{\rho}_{\boldsymbol{q}}(\tau)\hat{\rho}^{\dagger}_{\boldsymbol{q}}\rangle$ for a 2D system of 5 noninteracting spinless fermions. Such mismatch arises from the imposition of the ground state nodal structure as a subset of the nodal structure of all excited states.

It is thus very interesting to investigate the accuracy of the imaginary time correlation functions calculated by QMC using nodal restrictions different from FN.

In recent years alternative QMC methods have been conceived, which simulate the imaginary time evolution with a suitable stochastic process taking place in the manifold of Slater determinants.[18,21–23,25] In the present work we consider one of such QMC methods, the phaseless Auxiliary Field Quantum Monte Carlo (AFQMC),[21,23,26] which is considered less sensitive than FN to the quality of the trial function.[31] However, the phaseless approximation is less known than those characterizing configuration QMC methods, and its accuracy in the calculation of imaginary time correlation functions is unknown. We give a detailed description of AFQMC and present its application to the calculation of imaginary time correlation functions. To assess the accuracy of the phaseless AFQMC we compute ITCFs for a class of interacting fermionic models amenable to exact diagonalization of the hamiltonian.

The phaseless AFQMC and its extension to the calculation of imaginary time dynamics are described in Sec. II. The solvable fermionic systems are presented in Sec. III. Results of numeric calculations are presented in Sec. IV, and conclusions are drawn in Sec. V.

II. THE PHASELESS AFQMC

As mentioned in the Introduction, Quantum Monte Carlo are *ab initio*: this means that the starting point is the Hamiltonian operator of a physical system. We thus present the phaseless AFQMC relying on a very general hamiltonian operator:

$$\hat{H} = \sum_{i,j=1}^{M} \beta_{ij}\, \hat{a}_i^{\dagger}\hat{a}_j + \sum_{i,j,k,l=1}^{M} \gamma_{ijlk}\, \hat{a}_i^{\dagger}\hat{a}_j^{\dagger}\hat{a}_k\hat{a}_l. \qquad (1)$$

The creation and destruction operators appearing in (1) are related to an orthonormal complete set of orbitals $\{|\varphi_i\rangle\}_{i=1}^{M}$ in the single-particle Hilbert space, which we will denote $\mathcal{H}$. M is the dimension of such Hilbert space; we will make the assumption that $M < +\infty$. The above written Hamiltonian operator acts on the fermionic Fock space, $\mathcal{F}$, built upon the one body space $\mathcal{H}$. Throughout this paper, we will fix the number

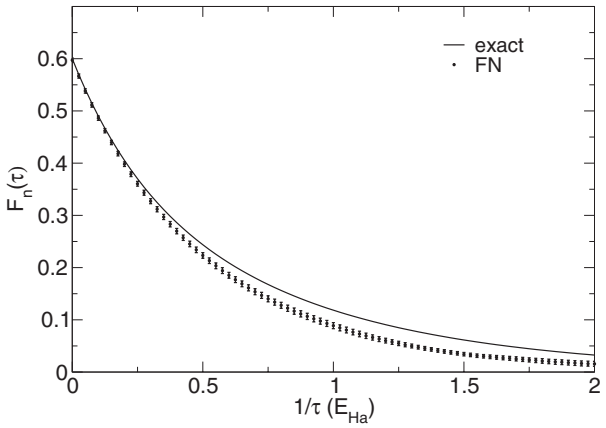

FIG. 1. FN result (points) and exact value (line) of the imaginary time correlation function of $\hat{\rho}_{\boldsymbol{q}}$ with $\boldsymbol{q} = \frac{2\pi}{L}(0, 1)$ for a 2D system of 5 noninteracting spinless fermions. Details of the calculation are presented in Appendix B.

of particles N, which is a constant of motion for (1). Within the N-particles subspace of the Fock space $\mathcal{F}$, the operator $\hat{H}$ has the spectral resolution:

$$\hat{H} = \sum_{\alpha} \epsilon_{\alpha} |\Phi_{\alpha}\rangle\langle\Phi_{\alpha}|, \tag{2}$$

where $\{\epsilon_{\alpha}\}_{\alpha}$ are the eigenvalues and $\{|\Phi_{\alpha}\rangle\}_{\alpha}$ the eigenvectors. Naturally the above expression is N-dependent, but we will not include an explicit label N to simplify the notation. The sum over α ranges from 0 to the dimension of the N-body fermionic space, equal to $\binom{M}{N}$. While zero temperature equilibrium properties of an N-particle system are completely determined by the ground state of (1), $|\Phi_0\rangle$, the study of dynamic properties requires knowledge of the spectrum $\{\epsilon_{\alpha}\}_{\alpha}$. Throughout the present work we shall make the technical assumption that $\epsilon_0 < \epsilon_1 \leq \ldots$, i.e., the N-particle ground state is non-degenerate.

A wide class of QMC methods relies on the observation that the imaginary time propagator

$$e^{-\tau\hat{H}}, \quad \tau \geq 0 \tag{3}$$

enables the ground state of an N-particle system to be recovered. In fact, as long as a trial state $|\Psi_T\rangle$ has non-zero overlap with $|\Phi_0\rangle$ the following relation holds:

$$\lim_{\tau\to\infty} e^{-\tau(\hat{H}-\epsilon_0)}|\Psi_T\rangle = |\Phi_0\rangle\langle\Phi_0|\Psi_T\rangle, \tag{4}$$

where the unknown quantity ϵ_0 is replaced with an *adaptive* estimate, according to a common procedure in Diffusion Monte Carlo (DMC) calculations.[16] QMC methods rely on the observation that deterministic evolution driven by the family of operators (3) can be mapped onto suitable stochastic processes and solved by randomly sampling appropriate probability distributions.

Along with the typical approach in which (4) is associated with a diffusion process in the configurational space of the system,[4,5,16] in a class of more recently developed QMC methods, the so-called *determinantal*[18,19,21–23] methods, (4) is mapped onto a stochastic process in the abstract manifold, which we will denote $\mathfrak{D}(N)$, of N-particle Slater determinants.

In AFQMC,[20–24,26,28–30] the association between (4) and a stochastic process in $\mathfrak{D}(N)$ is made possible by a discretization:

$$e^{-\tau(\hat{H}-\epsilon_0)} = (e^{-\delta\tau(\hat{H}-\epsilon_0)})^n, \tag{5}$$

with $\delta\tau = \frac{\tau}{n}$, and by a combined use of the Trotter-Suzuki decomposition of the propagator[32,33] and of the *Hubbard-Stratonovich transformation*[26,34,35] on the factors $e^{-\delta\tau(\hat{H}-\epsilon_0)}$. The Hubbard-Stratonovich transformation is an operator identity guaranteeing that

$$e^{-\delta\tau(\hat{H}-\epsilon_0)} = \int dg(\boldsymbol{\eta})\, \hat{G}(\boldsymbol{\eta}) + \mathcal{O}(\delta\tau^2), \tag{6}$$

with $dg(\boldsymbol{\eta})$ standard $2M^2$-dimensional normal probability measure, $\hat{G}(\boldsymbol{\eta}) = e^{\hat{A}(\boldsymbol{\eta})}$ and $\hat{A}(\boldsymbol{\eta}) = \sum_{i,j=1}^{M} \mathcal{A}(\boldsymbol{\eta})_{i,j}\hat{a}_i^{\dagger}\hat{a}_j$ a suitable *one-particle operator*, the structure of which is discussed in detail in Appendix A 2.

Equation (6) establishes a formal correspondence between an interacting fermion system and an ensemble of *non-interacting* fermion systems subject to *fluctuating external potentials*. The coupling with these external potentials is controlled by normally distributed parameters $\boldsymbol{\eta}$, called *auxiliary fields*, integration over which recovers the interaction.

To quantitatively realize that (6) provides a random walk representation of the imaginary time evolution, let us consider the stochastic process defined by the succession of wave functions:

$$|\Psi_n\rangle = \hat{G}(\boldsymbol{\eta}_{n-1})\ldots\hat{G}(\boldsymbol{\eta}_0)|\Psi_T\rangle, \tag{7}$$

where the operators $\hat{G}(\boldsymbol{\eta}_k)$ are functions of independent normally distributed random variables $\boldsymbol{\eta}_k$. It is known, and will be shown in details in Appendix A 1, that, if $|\Psi_T\rangle \in \mathfrak{D}(N)$, all the random variables $|\Psi_n\rangle$ take values in $\mathfrak{D}(N)$. Furthermore, their average is given by

$$\begin{aligned}\langle|\Psi_n\rangle\rangle_{\boldsymbol{\eta}_{n-1}\ldots\boldsymbol{\eta}_0} &= \langle\hat{G}(\boldsymbol{\eta}_{n-1})\ldots\hat{G}(\boldsymbol{\eta}_0)\rangle_{\boldsymbol{\eta}_{n-1}\ldots\boldsymbol{\eta}_0}|\Psi_T\rangle \\ &= \int dg(\boldsymbol{\eta}_{n-1})\ldots dg(\boldsymbol{\eta}_0)\,\hat{G}(\boldsymbol{\eta}_{n-1})\ldots\hat{G}(\boldsymbol{\eta}_0)|\Psi_T\rangle \\ &= e^{-n\delta\tau(\hat{H}-\epsilon_0)}|\Psi_T\rangle + \mathcal{O}(\delta\tau^2).\end{aligned} \tag{8}$$

Expression (8) clearly shows that the solution of the imaginary time Schrödinger equation (4) can be recovered as average of a suitable stochastic process, the structure of which is suggested by (7). Combining (4) and (7) it is evident that numerical sampling of such stochastic process provides a stochastic linear combination of Slater determinants, representing an estimation of the ground state of (1). The most natural choice of the trial function $|\Psi_T\rangle$, which we will use throughout the present work, is the Hartree-Fock ground state of the Hamiltonian, i.e., the lowest energy Slater determinant.

A. Control of the fermion sign problem: The phaseless AFQMC

Despite its formal simplicity, the straightforward numerical implementation leads in general to an exponential increase

in statistical errors with the imaginary time, due to the fact that complex random phases appear during the evolution (4).

S. Zhang invented a modification of the stochastic process through the introduction of an importance sampling transformation[26] that *guides* the random walk, closely resembling the typical scheme adopted[17] in configurational DMC simulations. The state $e^{-n\delta\tau(\hat{H}-\epsilon_0)}|\Psi_T\rangle$ is rewritten in the following form, detailed in Appendix A 3 and equivalent to (8):

$$\begin{aligned} & e^{-n\delta\tau(\hat{H}-\epsilon_0)}|\Psi_T\rangle \\ & \simeq \int dg(\boldsymbol{\eta}_{n-1})\ldots dg(\boldsymbol{\eta}_0) \\ & \quad \times \mathfrak{W}[\boldsymbol{\eta}_{n-1}, \boldsymbol{\xi}_{n-1}\ldots\boldsymbol{\eta}_0, \boldsymbol{\xi}_0] \\ & \quad \times \frac{\hat{G}(\boldsymbol{\eta}_{n-1}-\boldsymbol{\xi}_{n-1})\ldots\hat{G}(\boldsymbol{\eta}_0-\boldsymbol{\xi}_0)|\Psi_T\rangle}{\langle\Psi_T|\hat{G}(\boldsymbol{\eta}_{n-1}-\boldsymbol{\xi}_{n-1})\ldots\hat{G}(\boldsymbol{\eta}_0-\boldsymbol{\xi}_0)|\Psi_T\rangle}, \end{aligned} \tag{9}$$

where *complex-valued shift parameters* $\boldsymbol{\xi}_{n-1}\ldots\boldsymbol{\xi}_0$ and a weight function have been inserted. The latter satisfies the recursion relation:

$$\begin{aligned} & \mathfrak{W}[\boldsymbol{\eta}_n, \boldsymbol{\xi}_n\ldots\boldsymbol{\eta}_0, \boldsymbol{\xi}_0] \\ & = \mathfrak{W}[\boldsymbol{\eta}_{n-1}, \boldsymbol{\xi}_{n-1}\ldots\boldsymbol{\eta}_0, \boldsymbol{\xi}_0] \\ & \quad \times \mathfrak{I}[\boldsymbol{\eta}_n, \boldsymbol{\xi}_n; \hat{G}(\boldsymbol{\eta}_{n-1}-\boldsymbol{\xi}_{n-1})\ldots\hat{G}(\boldsymbol{\eta}_0-\boldsymbol{\xi}_0)|\Psi_T\rangle], \end{aligned} \tag{10}$$

where the following *importance function*:

$$\mathfrak{I}[\boldsymbol{\eta}, \boldsymbol{\xi}; |\Psi\rangle] = e^{-\frac{\boldsymbol{\xi}\cdot\boldsymbol{\xi}}{2}-\boldsymbol{\eta}\cdot\boldsymbol{\xi}}\frac{\langle\Psi_T|\hat{G}(\boldsymbol{\eta}-\boldsymbol{\xi})|\Psi\rangle}{\langle\Psi_T|\Psi\rangle} \tag{11}$$

appears. The shift parameters are chosen to minimize fluctuations in the importance function to first order in $\delta\tau$. The importance sampling expression (11) clearly shows the mechanism responsible for the appearance of the sign problem in the framework of AFQMC: *when the overlap between one or more walkers and the trial state vanishes* massive fluctuations in the importance function occur, determining *drastic statistical errors in the AFQMC estimate* (9) for the solution of (4). In the method conceived by S. Zhang, the *exact* complex-valued importance function appearing in (11) is replaced[23] by the approximate form:

$$\mathfrak{I}[\boldsymbol{\eta}, \boldsymbol{\xi}; |\Psi\rangle] \simeq e^{-\delta\tau(\epsilon_{loc}(\Psi)-\epsilon_0)} \times \max(0, \cos(\Delta\theta)), \tag{12}$$

where $\epsilon_{loc}(\Psi) = \mathrm{Re}[\frac{\langle\Psi_T|\hat{H}|\Psi\rangle}{\langle\Psi_T|\Psi\rangle}]$ is the *local energy* functional, and

$$\Delta\theta = \mathrm{Im}\left[\log\left[\frac{\langle\Psi_T|\hat{G}(\boldsymbol{\eta}-\boldsymbol{\xi})|\Psi\rangle\rangle}{\langle\Psi_T|\Psi\rangle}\right]\right]. \tag{13}$$

The derivation of such approximate form is detailed in Appendix A 3. The first factor corresponds to the so-called *real local energy approximation*, which turns (11) into a *real quantity*, avoiding typical phase problems arising from complex weights. The second factor, together with the introduction of the shift parameters, has been argued in Refs. 23 and 26 to keep the overlap between the determinants involved in the random walk and the trial determinant far from zero. In fact, the angle $\Delta\theta$ corresponds to the flip in the phase of a determinant during a step of the random walk: the term $\max(0, \cos(\Delta\theta))$ is meant to suppress determinants whose phase undergoes an abrupt change, under the assumption[23,26] that such behavior indicates the vanishing of the overlap with the trial state.

Equation (9), together with the choice (12) for the evolution of the weights attached to the Slater determinants, gives rise to the so-called *phaseless AFQMC method*.

The underlying approximation is known to be good for the ground state, but ITCFs require sampling of excited states, related to the fluctuations around the asymptotic distribution of the random walk: this issue is largely unexplored, and the aim of the present work is to address its accuracy. There is no *a priori* motivation for concluding that the approximation (12) is better than the FN for the exploration of the manifold of excited states. One of the topics investigated in the present work is the verification of this important point for a model system by comparison with exact results.

We stress that the complex weights and the vanishing of the overlap with the trial state, responsible for the appearance of the sign problem in AFQMC, occur even for very small systems, such as two particles with opposite spins: for those systems, it is notoriously absent in configurational QMC

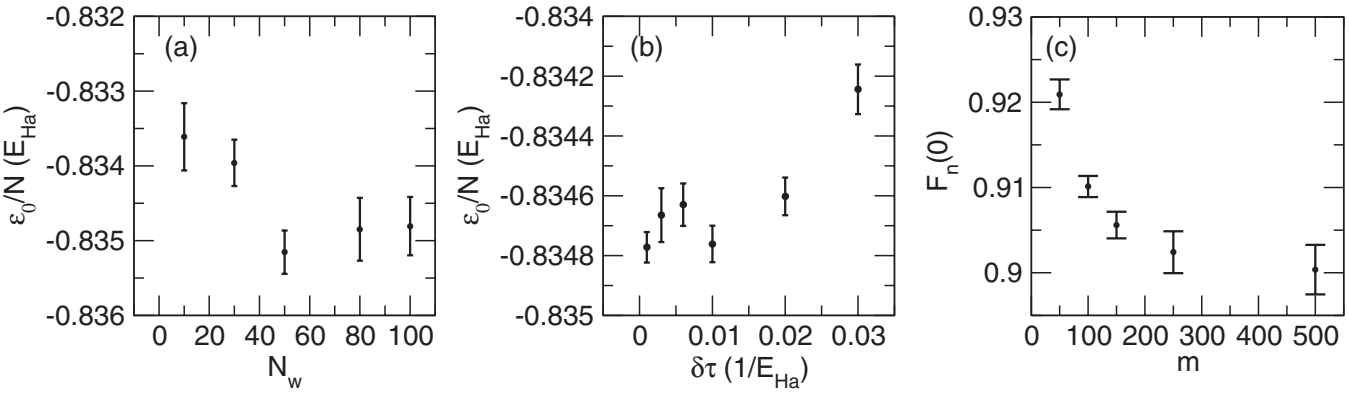

FIG. 2. Steps of the convergence procedure for $(N_\uparrow, N_\downarrow, r_s, M) = (1, 1, 1, 49)$: (a) AFQMC estimate of the ground state energy per particle for several values of N_w at fixed $\delta\tau = 0.001$: N_w can be safely set to 80. (b) AFQMC estimate of the ground state energy per particle for several values of $\delta\tau$ at fixed $N_w = 80$: $\delta\tau$ can be safely set to 0.003. (c) AFQMC estimate of $F_{\mathbf{n}}(0)$ for several values of m at fixed $N_w = 80$, $\delta\tau = 0.003$: m can be safely set to 250.

methods, since the spatial part of the wave function is symmetric and positive.

B. The algorithm

The so-far introduced observations give rise to a *polynomially complex* algorithm for numerically sampling the solution (4), the efficiency of which relies on the observation that the walkers $|\Psi_k^{(w)}\rangle$ lie in $\mathfrak{D}(N)$ and can be therefore parametrized with an $M \times N$ complex-valued matrix, as discussed in Appendix A 1. The algorithm can be resumed in the following sequence of operations:

1. A collection $|\Psi_0^{(1)}\rangle \dots |\Psi_0^{(N_w)}\rangle$ of Slater determinants, henceforth referred to as *walkers*, is initialized to a trial state $|\Psi_T\rangle$.
2. For $k = 0 \dots n-1$ an adaptive estimate of the ground state energy is produced according to the formula:

$$\epsilon_0 \simeq \frac{1}{\sum_{w=1}^{N_w} \mathfrak{W}_k^{(w)}} \sum_{w=1}^{N_w} \mathfrak{W}_k^{(w)} \frac{\langle \Psi_T | \hat{H} | \Psi_k^{(w)} \rangle}{\langle \Psi_T | \Psi_k^{(w)} \rangle}, \tag{14}$$

normally distributed auxiliary field configurations $\boldsymbol{\eta}_k^{(1)} \dots \boldsymbol{\eta}_k^{(N_w)}$ are sampled, and walkers and weights are updated according to

$$\begin{aligned} |\Psi_{k+1}^{(w)}\rangle &= \hat{G}(\boldsymbol{\eta}_k^{(w)} - \boldsymbol{\xi}_k^{(w)}) |\Psi_k^{(w)}\rangle, \\ \mathfrak{W}_{k+1}^{(w)} &= \mathfrak{W}_k^{(w)} \mathfrak{I}[\boldsymbol{\eta}_k^{(w)}, \boldsymbol{\xi}_k^{(w)}; |\Psi_k^{(w)}\rangle]. \end{aligned} \tag{15}$$

3. An estimate for $e^{-n\delta\tau(\hat{H}-\epsilon_0)}|\Psi_T\rangle$ is given by

$$e^{-n\delta\tau(\hat{H}-\epsilon_0)}|\Psi_T\rangle \simeq \sum_{w=1}^{N_w} \mathfrak{W}_n^{(w)} \frac{|\Psi_n^{(w)}\rangle}{\langle \Psi_T | \Psi_n^{(w)} \rangle}. \tag{16}$$

The ground state average $\langle \Phi_0 | \hat{O} | \Phi_0 \rangle$ of a many-body observable $\hat{O}$ not commuting with $\hat{H}$ is the $m, n \to \infty$ limit of the following formula:

$$\frac{\langle \Psi_T | e^{-m\delta\tau(\hat{H}-\epsilon_0)} \hat{O} e^{-n\delta\tau(\hat{H}-\epsilon_0)} | \Psi_T \rangle}{\langle \Psi_T | e^{-(m+n)\delta\tau(\hat{H}-\epsilon_0)} | \Psi_T \rangle} \tag{17}$$

for which manipulations analogous to the importance sampling transformation, discussed in detail in Appendix A 4, yield the following *backpropagated*[27] estimate:

$$\langle \Phi_0^{(N)} | \hat{O} | \Phi_0^{(N)} \rangle \simeq \frac{\sum_{w=1}^{N_w} \mathfrak{W}_{n+m}^{(w)} \frac{\langle \Psi_{BP,m}^{(w)} | \hat{O} | \Psi_n^{(w)} \rangle}{\langle \Psi_{BP,m}^{(w)} | \Psi_n^{(w)} \rangle}}{\sum_{w=1}^{N_w} \mathfrak{W}_{n+m}^{(w)}}, \tag{18}$$

with

$$\begin{aligned} |\Psi_n^{(w)}\rangle &= \hat{G}(\boldsymbol{\eta}_{n-1} - \boldsymbol{\xi}_{n-1}) \dots \hat{G}(\boldsymbol{\eta}_0 - \boldsymbol{\xi}_0) |\Psi_T\rangle, \\ |\Psi_{BP,m}^{(w)}\rangle &= \hat{G}^\dagger(\boldsymbol{\eta}_n - \boldsymbol{\xi}_n) \dots \hat{G}^\dagger(\boldsymbol{\eta}_{n+m-1} - \boldsymbol{\xi}_{n+m-1}) |\Psi_T\rangle. \end{aligned} \tag{19}$$

Notice that the backpropagation technique is necessary to obtain ground state averages from the random walk. In the absence of backpropagation, only *mixed estimates* of the form $\frac{\langle \Psi_T | \hat{O} | \Phi_0 \rangle}{\langle \Psi_T | \Phi_0 \rangle}$ can be obtained, which coincide with ground state

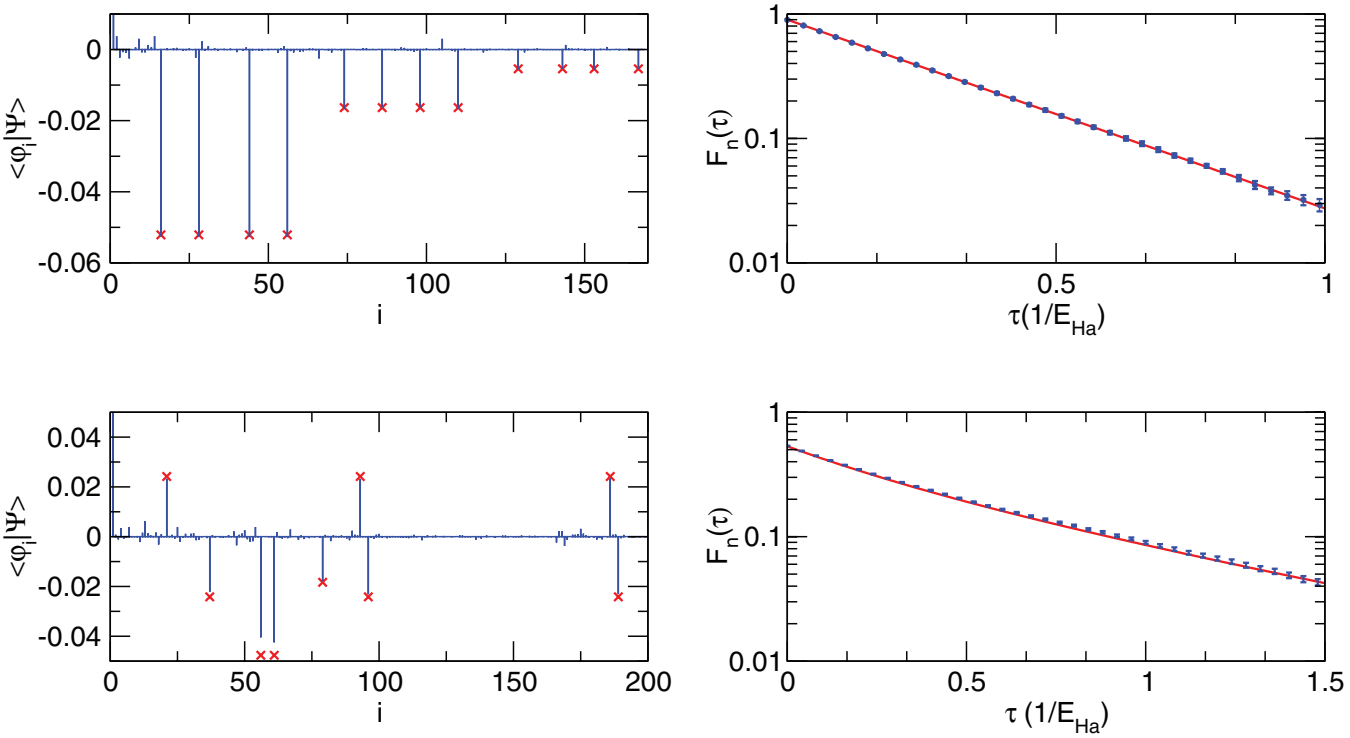

FIG. 3. Left column: exact nonvanishing (red crosses) and reconstructed (blue columns) components of the ground state for systems with $N_\uparrow, N_\downarrow = (1, 1)$, $(5, 0)$ (top to bottom), relative to all elements of the basis except $|\varphi_1\rangle = |\Psi_T\rangle$. Exact and reconstructed values of $\langle \varphi_1 | \Psi \rangle$ are, respectively, 0.9937, 0.9939(2) and 0.9926, 0.9885(3). Right column: exact (red line) and reconstructed (circles) imaginary time correlation function of the density fluctuation operator with $\mathbf{n} = (1, 0)$ for systems with $N_\uparrow, N_\downarrow = (1, 1)$, $(5, 0)$ (top to bottom). When not visible, error bars are smaller than the symbol size.

TABLE I. Exact (column 6) and calculated (column 5) ground state energy per particle in Hartree units, and overlap between exact and reconstructed ground state (column 7) for various systems (parameters are listed in columns 1 to 4).

$N_\uparrow$	$N_\downarrow$	r_s	M	ϵ_0/N(*AFQMC*)	ϵ_0/N(*exact*)	$\langle\Phi_0\vert\Psi\rangle$
1	1	1	5	−0.82255(5)	−0.82259	0.99999(5)
1	1	1	13	−0.8315(1)	−0.8313	0.9999(1)
1	1	1	21	−0.83338(6)	−0.83307	0.9989(7)
1	1	1	49	−0.83476(7)	−0.83441	0.9882(4)
1	1	2	5	−0.4282(1)	−0.4282	0.9629(3)
1	1	2	13	−0.4351(1)	−0.4330	0.9650(2)
1	1	2	21	−0.4359(3)	−0.4339	0.9586(2)
1	1	2	49	−0.4362(3)	−0.4345	0.9594(5)
1	1	3	21	−0.3020(3)	−0.2972	0.9253(8)
1	1	4	21	−0.2320(4)	−0.2272	0.904(1)
5	0	1	9	0.11327(2)	0.11247	0.99185(1)
5	0	1	13	0.10726(3)	0.10591	0.98600(7)
5	0	2	9	−0.19485(1)	−0.19751	0.9863(4)
5	0	2	13	−0.19878(2)	−0.20311	0.9683(3)

expectations (17) only if $\hat{O}$ commutes with the Hamiltonian $\hat{H}$.

C. Imaginary time correlation functions

In a well-established approach[7–12,19] to the reconstruction of dynamic properties of many body systems, the *dynamic structure factor* of the single-particle operators $\hat{A}$, $\hat{B}$:

$$S_{\hat{A},\hat{B}}(\omega) = \int_{\mathbb{R}} dt\, \frac{e^{i\omega t}}{2\pi} \langle\Phi_0|\hat{A}(t)\hat{B}|\Phi_0\rangle \tag{20}$$

is recovered from their *imaginary time correlation function*:

$$F_{\hat{A},\hat{B}}(\tau) = \frac{\langle\Phi_0|\hat{A}(\tau)\hat{B}|\Phi_0\rangle}{N} = \frac{\langle\Phi_0|\hat{A}e^{-\tau(\hat{H}-\epsilon_0)}\hat{B}|\Phi_0\rangle}{N} \tag{21}$$

though a numeric inverse Laplace transform. Being constructed with the imaginary time evolution operator, the ITCF (21) is a natural quantity to be evaluated in QMC calculations. Its evaluation in determinantal QMC methods, however, is not as simple as in configurational QMC: straightforward extension of the backpropagation technique to the evaluation of (21) is in fact prevented because the single-particle

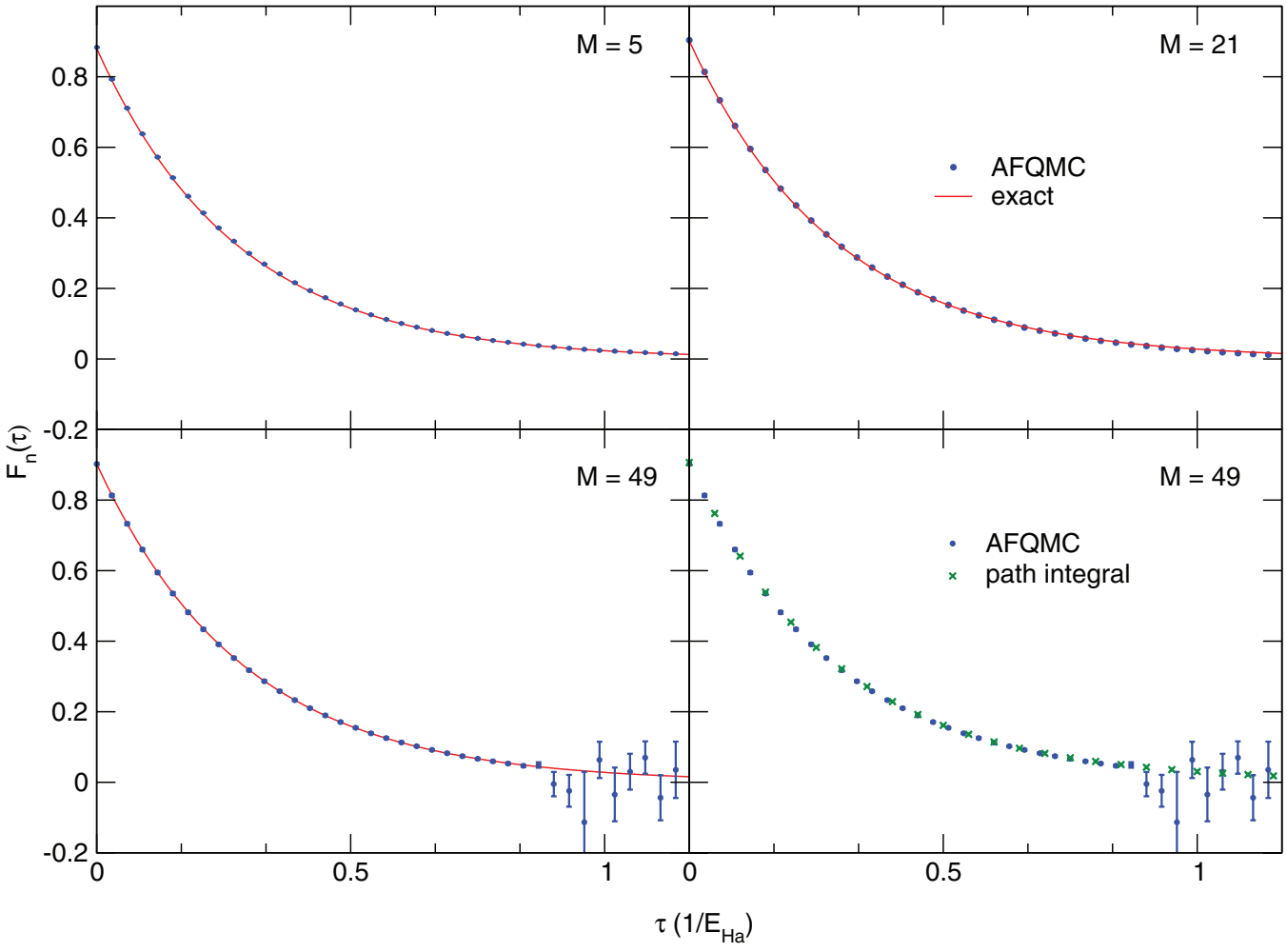

FIG. 4. Imaginary time correlation function of the momentum shift operator relative to $M = 5, 21, 49$ at $r_s = 1$ for $N_\uparrow = 1$, $N_\downarrow = 1$. In the right lower box, comparison between AFQMC and exact Path Integral QMC calculations is given. When not visible, error bars are smaller than the symbol size.

operator $\hat{B}$ does not preserve $\mathfrak{D}(N)$. To overcome this difficulty, we generalize the clever approach conceived by Feldbacher and Assaad[24] for the calculation of dynamical Green functions: we introduce the Hubbard-Stratonovich representation (6) of the imaginary time propagator in (21) and move the operators $\hat{G}(\boldsymbol{\eta})$ to the right of $\hat{B} = \sum_{ij=1}^{M} \mathcal{B}_{ij}\, \hat{a}_i^\dagger \hat{a}_j$ commuting them with the operators $\hat{a}_i^\dagger$, $\hat{a}_j$. As discussed in detail in Appendix A 5, this procedure determines the appearance of two random matrices in the estimator for (21):

$$\begin{aligned} F_{\hat{A},\hat{B}}(r\delta\tau) &= \frac{1}{N}\sum_{kl}\mathcal{B}_{kl}\int dg(\boldsymbol{\eta}_{n-1})\ldots dg(\boldsymbol{\eta}_{n-r}) \\ &\quad\times\langle\Phi_0|\hat{A}\hat{G}(\boldsymbol{\eta}_{n-1})\ldots\hat{G}(\boldsymbol{\eta}_{n-r})\hat{a}_k^\dagger\hat{a}_l|\Phi_0\rangle \\ &= \frac{1}{N}\sum_{ijkl}\mathcal{B}_{kl}\int dg(\boldsymbol{\eta}_{n-1})\ldots dg(\boldsymbol{\eta}_{n-r}) \\ &\quad\times\langle\Phi_0|\hat{A}\hat{a}_i^\dagger\hat{a}_j\hat{G}(\boldsymbol{\eta}_{n-1})\ldots\hat{G}(\boldsymbol{\eta}_{n-r})|\Phi_0\rangle \\ &\quad\times\mathcal{D}(\boldsymbol{\eta}_{n-1},\ldots,\boldsymbol{\eta}_{n-r})_{ik}\,\mathcal{D}^{-1}(\boldsymbol{\eta}_{n-1},\ldots,\boldsymbol{\eta}_{n-r})_{lj}, \end{aligned} \tag{22}$$

where $\mathcal{D}(\boldsymbol{\eta}_{n-1},\ldots,\boldsymbol{\eta}_{n-r}) = e^{\mathcal{A}(\boldsymbol{\eta}_{n-1})}\ldots e^{\mathcal{A}(\boldsymbol{\eta}_{n-r})}$.

Further application of the importance sampling transformation and of the backpropagation technique yields, as explained in Appendix A 5:

$$\begin{aligned} F_{\hat{A},\hat{B}}(r\delta\tau) &\simeq \frac{1}{N}\frac{1}{\sum_{w=1}^{N_w}\mathfrak{W}_{m+n-r}^{(w)}}\sum_{w=1}^{N_w}\sum_{ijkl}\mathcal{B}_{kl}\,\mathfrak{W}_{m+n}^{(w)} \\ &\quad\times\frac{\langle\Psi_{BP,m}^{(w)}|\hat{A}\hat{a}_i^\dagger\hat{a}_j|\Psi_n^{(w)}\rangle}{\langle\Psi_{BP,m}^{(w)}|\Psi_n^{(w)}\rangle} \\ &\quad\times\mathcal{D}\big(\boldsymbol{\eta}_{n-1}^{(w)}-\boldsymbol{\xi}_{n-1}^{(w)},\ldots,\boldsymbol{\eta}_{n-r}^{(w)}-\boldsymbol{\xi}_{n-r}^{(w)}\big)_{ik} \\ &\quad\times\mathcal{D}^{-1}\big(\boldsymbol{\eta}_{n-1}^{(w)}-\boldsymbol{\xi}_{n-1}^{(w)},\ldots,\boldsymbol{\eta}_{n-r}^{(w)}-\boldsymbol{\xi}_{n-r}^{(w)}\big)_{lj}. \end{aligned} \tag{23}$$

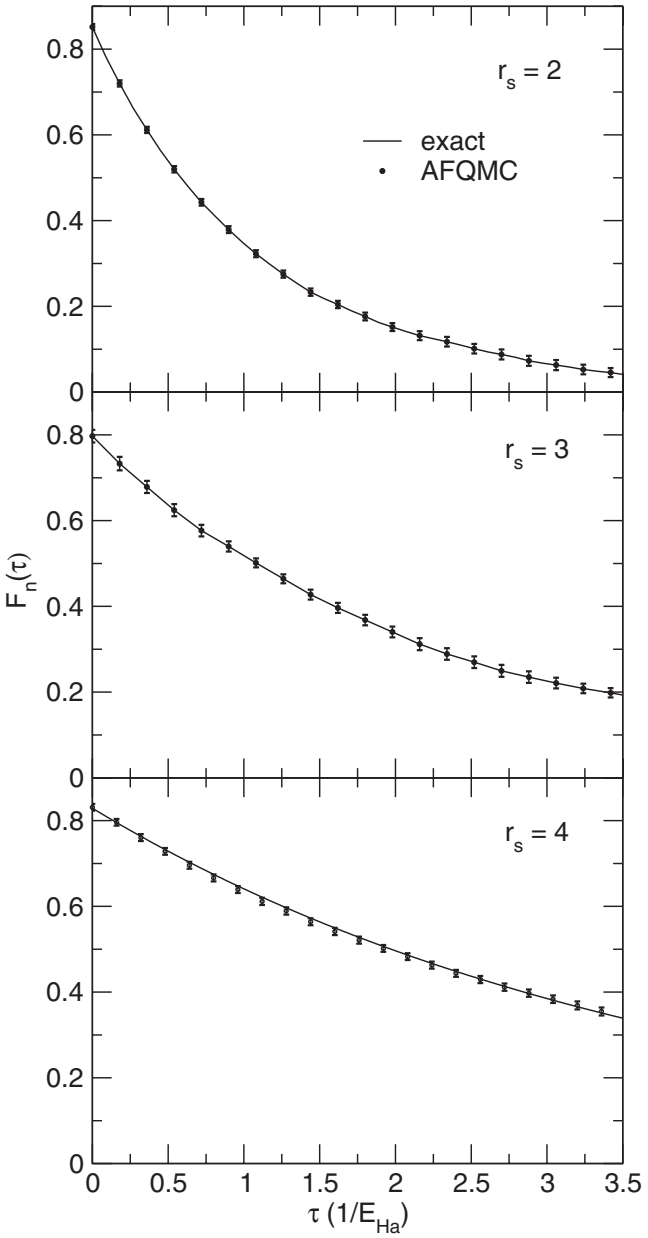

FIG. 5. Imaginary time correlation function of the momentum shift operator relative to $r_s = 2, 3, 4$ (top to bottom) for $N_\uparrow = 1, N_\downarrow = 1$ at $M = 21$. When not visible, error bars are smaller than the symbol size.

III. A CLASS OF SOLVABLE SYSTEMS

We test the accuracy of the AFQMC results on a class of simple systems for which exact numeric expression for the spectral decomposition (2) of the Hamiltonian operator $\hat{H}$ can be given. Let us consider the Hamiltonian of the 2D electron gas,

$$\begin{aligned} \hat{H} &= \frac{\xi\sqrt{N}}{\sqrt{4\pi}r_s} + \sum_{m,\sigma}\frac{2\pi}{N}\frac{|\boldsymbol{n}_m|^2}{r_s^2}\hat{a}_{m,\sigma}^\dagger\hat{a}_{m,\sigma} \\ &\quad+\sum_{\sigma,\sigma'}\sum_{mnrs}\frac{1}{\sqrt{4N\pi}\,r_s}\frac{\delta_{\boldsymbol{n}_r-\boldsymbol{n}_m,\boldsymbol{n}_n-\boldsymbol{n}_s}}{|\boldsymbol{n}_r-\boldsymbol{n}_m|}\hat{a}_{m,\sigma}^\dagger\hat{a}_{n,\sigma'}^\dagger\hat{a}_{s,\sigma'}\hat{a}_{r,\sigma}, \end{aligned} \tag{24}$$

where the single-particle Hilbert space $\mathcal{H}$ is spanned by the plane wave orbitals $|\boldsymbol{n}_i\sigma\rangle$ with $\boldsymbol{n}_i \in \mathbb{Z}^2$, $|\boldsymbol{n}_i|^2 \le n_{max}$ for some integer n_{max} and $\sigma = \pm 1$. The parameter $r_s \in (0, \infty)$ controls the relevance of the interaction part and N stands for the number of particles, and the constant $\xi = -3.900265$ arises from an Ewald summation procedure.[37] For small number of particles N and low kinetic energy cutoff n_{max} the above Hamiltonian defines a simple model which can be solved exactly.[38,39]

Knowledge of eigenvalues $\{\epsilon_\alpha\}_\alpha$ and eigenvectors $\{|\Phi_\alpha\rangle\}_\alpha$ of $\hat{H}$ allows exact calculation of the imaginary time propagator:

$$e^{-\tau(\hat{H}-\epsilon_0)} = \sum_\alpha e^{-\tau(\epsilon_\alpha-\epsilon_0)}|\Phi_\alpha\rangle\langle\Phi_\alpha|, \tag{25}$$

of the projector $|\Phi_0\rangle\langle\Phi_0|$ onto the minimum energy eigenspace, of backpropagated ground state averages:

$$\frac{\langle\Psi_T|e^{-m\delta\tau(\hat{H}-\epsilon_0)}\hat{O}|\Phi_0\rangle}{\langle\Psi_T|e^{-m\delta\tau(\hat{H}-\epsilon_0)}|\Phi_0\rangle} = \frac{\sum_\alpha\langle\Psi_T|\Phi_\alpha\rangle e^{-m\delta\tau(\epsilon_\alpha-\epsilon_0)}\langle\Phi_\alpha|\hat{O}|\Phi_0\rangle}{\langle\Psi_T|\Phi_0\rangle} \tag{26}$$

and of backpropagated imaginary time correlation functions (21):

$$\begin{aligned} &F_{\hat{A},\hat{B}}(\tau) \\ &= \frac{1}{N}\frac{\langle\Psi_T|e^{-m\delta\tau(\hat{H}-\epsilon_0)}\hat{A}e^{-r\delta\tau(\hat{H}-\epsilon_0)}\hat{B}|\Phi_0\rangle}{\langle\Psi_T|e^{-m\delta\tau(\hat{H}-\epsilon_0)}|\Phi_0\rangle} \\ &= \frac{1}{N}\frac{\sum_{\alpha,\beta}\langle\Psi_T|\Phi_\alpha\rangle e^{-m\delta\tau(\epsilon_\alpha-\epsilon_0)-r\delta\tau(\epsilon_\beta-\epsilon_0)}\langle\Phi_\alpha|\hat{A}|\Phi_\beta\rangle\langle\Phi_\beta|\hat{B}|\Phi_0\rangle}{\langle\Psi_T|\Phi_0\rangle} \end{aligned} \tag{27}$$

and the comparison of such quantities with AFQMC results.

We focus on the ITCF $F_{\boldsymbol{n}}(\tau) = \frac{1}{N}\langle\Psi_0|\hat{\rho}_{\boldsymbol{n}}(\tau)\hat{\rho}_{-\boldsymbol{n}}|\Psi_0\rangle$ of the density fluctuation operator:

$$\hat{\rho}_{\boldsymbol{n}} = \sum_{i,j}\sum_\sigma \delta_{\boldsymbol{n}_i,\boldsymbol{n}_j-\boldsymbol{n}}\,\hat{a}^\dagger_{i,\sigma}\hat{a}_{j,\sigma} \tag{28}$$

and of its adjoint $\hat{\rho}^\dagger_{\boldsymbol{n}} = \hat{\rho}_{-\boldsymbol{n}}$.

IV. RESULTS

The phaseless AFQMC method represents the ground state as a stochastic linear combination of Slater determinants (16) from which accurate estimates of the ground state energy can be obtained.[22,26] However, much more information can be obtained from the simulation. Here we present results for the components of the ground state on the chosen basis of the Hilbert space and for the imaginary time correlation functions.

Each of the simulations presented below is characterized by two sets of parameters: ($N_\uparrow$, $N_\downarrow$, r_s, M) define the system under study, whereas ($\delta\tau$, m, N_w) control the details of the simulation. In particular, $N_\uparrow$ ($N_\downarrow$) is the number of spin-up (spin-down) fermions, r_s controls the strength of the

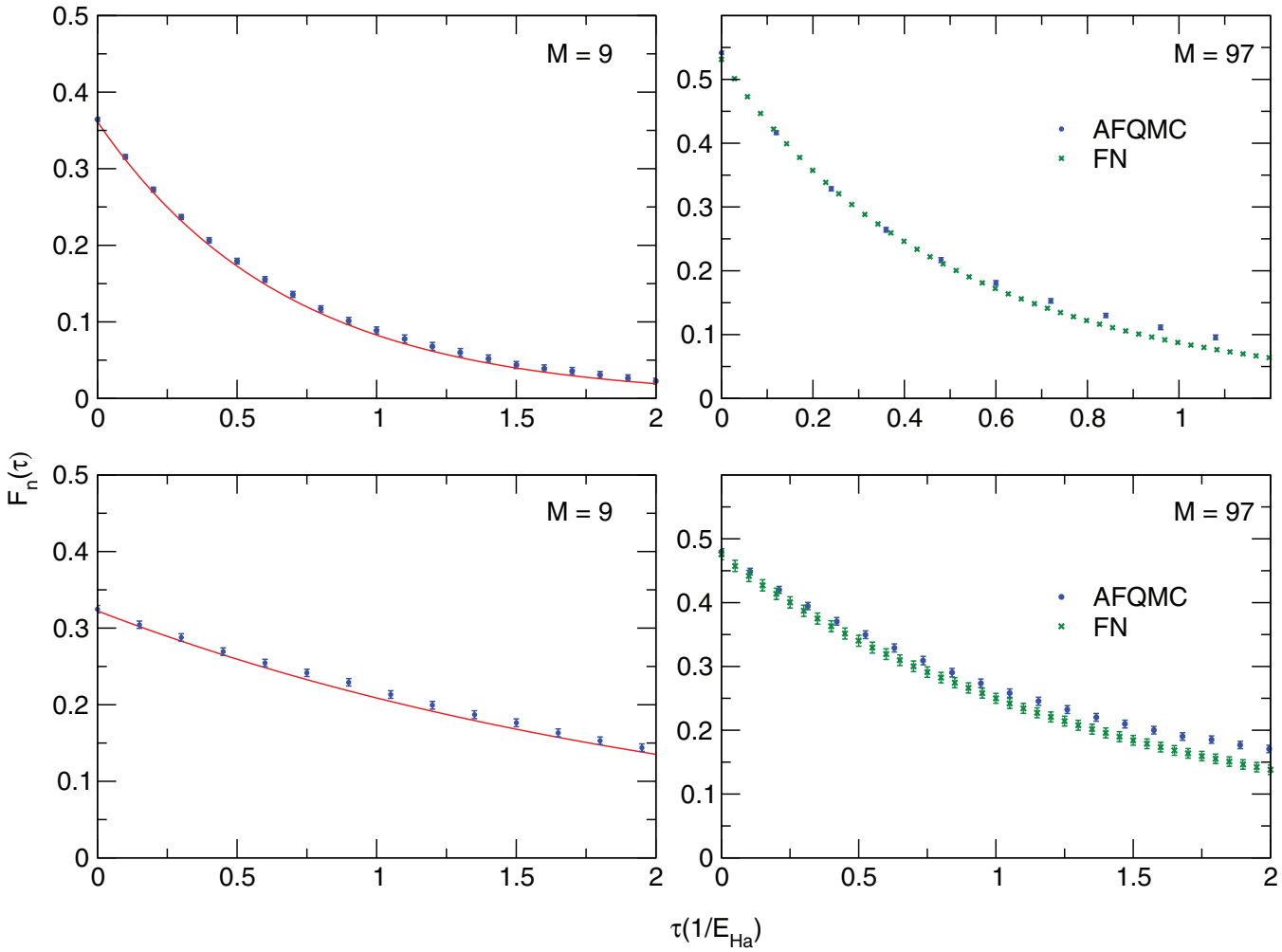

FIG. 6. Imaginary time correlation function of the momentum shift operator relative to $M = 9, 97$ at $r_s = 1$ (upper panel) and to $M = 13, 97$ at $r_s = 2$ (lower panel) for $N_\uparrow = 5$, $N_\downarrow = 0$. In the right box of each panel comparison between AFQMC and FN calculations (green crosses) is given. When not visible, error bars are smaller than the symbol size.

interaction, M fixes the order of the matrices with which the algorithm deals, while m corresponds to the number of back-propagation steps.

Apart from the basis set size M, which we keep small to allow comparison with exact diagonalization, and we extrapolate to the joint limit $\delta\tau \to 0$, $N_w \to \infty$,[36] and $m \to \infty$ to eliminate sources of systematic errors.

As an example, we show in Fig. 2 the extrapolations for a calculation with $(N_\uparrow, N_\downarrow, r_s, M) = (1, 1, 1, 49)$. Discrepancies with respect to the exact results are therefore due to the only uncontrolled approximations of the method, namely the *real local energy* and the *phase* approximations (12).

A. Assessment of the accuracy

In Fig. 3 we show results relative to the simulation of systems with $r_s = 1$, $M = 13$, for some values of $N_\uparrow$ and $N_\downarrow$. The left panels of Fig. 3 show the components of the stochastic solution on the Hilbert space basis functions. The little statistical fluctuations around the x axis show that the random walk visits a large number of states, while the significant components of the AFQMC solution match those of the exact ground state with good accuracy. The ITCF $F_{\boldsymbol{n}}(\tau)$ of the density fluctuation operator (28) for $\mathbf{n} = (1, 0)$ is reported in the right column of Fig. 3. The wave vector $\mathbf{n}$ has been chosen in the lowest energy shell since it gives rise to nonvanishing ITCFs even for small M. The agreement with exact values is remarkable, in particular if compared with the discrepancy observed for the FN result, Fig. 1: this constitutes the central result of the present work.

For all these systems we computed also the ground state energy per particle, and the overlap between exact and reconstructed ground state: the results are listed in Table I, the bias of the energy resulting of the order of $10^{-3}E_{Ha}$, which is smaller than the FN bias using a Slater-Jastrow trial function with plane-wave nodes.[41]

B. Computational issues

Although our primary interest is the assessment of the accuracy of AFQMC in calculating the ITCFs addressed in Sec. IV A, we explored the behavior of the method for larger values of r_s and M.

As r_s increases, the interaction becomes more and more important, and the overlap of the exact wave function with the trial function becomes smaller. Also the increase in M, which is required for the study of realistic models, makes the stochastic exploration of the Hilbert space more difficult: in particular, the calculation of ITCFs is further complicated by the need of multiplying many exponentials of large matrices, see (23), which induces instabilities at large imaginary time. This problem is already known in the literature.[24,42]

In Fig. 4 results appear relative to systems with $N_\uparrow = 1$, $N_\downarrow = 1$, showing that AFQMC estimations of static and dynamic properties remain in satisfactory agreement with exact values even if M is raised to 49. For $M = 49$ we are also in good agreement with exact Path Integral QMC calculations, providing the exact result in the limit $M \to +\infty$, which cannot be explored via exact diagonalization.

TABLE II. Values of $\chi^2 = \frac{1}{N_\tau}\sum_{i=1}^{N_\tau} \frac{|F_n^{(AFQMC)}(\tau_i) - F_n(\tau_i)|^2}{\sigma_i^2}$ for the various systems presented. N_τ is the number of imaginary time instants.

$N_\uparrow$	$N_\downarrow$	r_s	M	χ^2
1	1	1	5	1.02
1	1	1	13	0.02
1	1	1	21	0.09
1	1	1	49	0.04
1	1	2	5	0.97
1	1	2	21	0.90
1	1	2	49	0.32
1	1	3	21	0.05
1	1	4	21	0.70
5	0	1	9	0.69
5	0	1	13	2.87
5	0	2	9	1.09

The algorithm is able to reproduce exact values even at $r_s = 2$, 3, 4 and $M = 21$, as shown in Fig. 5. Since it is known that the degree of correlation in the uniform electron gas is significantly higher in 2D than in 3D for given r_s, the range of densities covered well represents the typical realistic density values in 3D (up to $r_s \sim 5$).

We complete the study with calculations relative to systems with $N_\uparrow, N_\downarrow = (5, 0)$. Results are shown in Fig. 6. For $M = 9$ the quality of AFQMC calculations is still satisfactory, even if we observe a small overestimate of $F_{\mathbf{n}}(\tau)$. Finally, for $M = 97$ we compared our results with FN calculations. We observe good agreement between the estimates of the static property $F_{\mathbf{n}}(0)$ yield by both algorithms. As far as finite τ ITCFs are concerned, we found that the discrepancy between the two results qualitatively resembles the discrepancy between exact solution and FN in the case of noninteracting particles in Fig. 1: an encouraging result.

To quantify the quality of the presented results, the reader may refer to Table II, where we report an average reduced chi-squared.

V. CONCLUSIONS

In the present work we gave a detailed description of the phaseless AFQMC algorithm, we proposed a scheme for its application to the calculation of dynamical properties of zero temperature fermion systems and we tested the methodology against exact diagonalization for interacting few fermion systems. Such tests revealed that it is actually possible to compute imaginary time correlation functions with satisfactory accuracy, at least for systems with moderate number of particles and interaction strength. This is a very interesting result since it is known that there exist situations when the well established and widely employed FN approximation scheme provides inaccurate results for ITCFs. The present work indicates that the AFQMC algorithm can become an accurate tool to calculate dynamical properties of few body systems. We hope that the accuracy of our results will encourage the development of technical tools necessary to study larger systems,

such as the numeric stabilization[40,42] of the products of matrix exponentials involved both in the backpropagation[27] and in the calculation of imaginary time correlation functions. In perspective, an accurate calculation of ITCFs is a prerequisite for the analytic continuation[7] leading to real-time dynamics of quantum systems.

ACKNOWLEDGMENTS

This work has been supported by Regione Lombardia and CINECA Consortium through a LISA Initiative (Laboratory for Interdisciplinary Advanced Simulation) 2012 grant (http://www.hpc.cineca.it/services/lisa), and by a grant *Dote ricerca*: FSE, Regione Lombardia.

APPENDIX A: ALGORITHMIC DETAILS

The aim of this appendix is completing the description of the extended AFQMC outlined in Sec. II.

1. Properties of Slater determinants

For a generic Slater determinant $|\Psi\rangle$ there exist single-particle orbitals $|\psi_1\rangle \dots |\psi_N\rangle \in \mathcal{H}$ for which $|\Psi\rangle = |\psi_1 \dots \psi_N\rangle_-$. As a consequence the state

$$\begin{aligned} |\Psi\rangle &= \sum_{i_1 \dots i_N} \langle \varphi_{i_1}|\psi_1\rangle \dots \langle \varphi_{i_N}|\psi_N\rangle |\varphi_{i_1} \dots \varphi_{i_N}\rangle_- \\ &= \sum_{i_1 \dots i_N} \frac{\Psi_{i_1 1} \dots \Psi_{i_N N}}{\sqrt{N!}} \hat{a}^\dagger_{i_1} \dots \hat{a}^\dagger_{i_N} |0\rangle \end{aligned} \tag{A1}$$

is completely and uniquely described by the $M \times N$ matrix $\Psi_{ij} = \langle \phi_i | \psi_j \rangle$.

In the light of such parametrization it can be proved[43] that for a generic N-particle Slater determinant $|\Psi\rangle$ and a generic one-body operator $\hat{O} = \sum_{i,j} \mathcal{O}_{ij} \hat{a}^\dagger_i \hat{a}_j$ the state $e^{\hat{O}}|\Psi\rangle$ is still a Slater determinant, described by the matrix $e^{\mathcal{O}}\Psi$, so that the manifold $\mathfrak{D}(N)$ of Slater determinants is closed under the action of exponentials of single-particle operators.

Equation (A1) also enables the concrete calculation overlaps and matrix elements of one-body and two-body operators. In particular, if $|\Psi\rangle$, $|\Phi\rangle$ are generic non-orthogonal N-particle Slater determinants the following properties[26,43,44] hold:

$$\begin{aligned} \langle \Phi|\Psi\rangle &= \frac{\det[\Phi^\dagger \Psi]}{N!}, \\ \frac{\langle \Phi|\hat{a}^\dagger_i \hat{a}_j|\Psi\rangle}{\langle \Phi|\Psi\rangle} &= \left[\Psi \left[\Phi^\dagger \Psi\right] \Phi^\dagger\right]_{ji} = \mathcal{G}_{ij}, \\ \frac{\langle \Phi|\hat{a}^\dagger_i \hat{a}^\dagger_j \hat{a}_k \hat{a}_l|\Psi\rangle}{\langle \Phi|\Psi\rangle} &= \mathcal{G}_{il}\mathcal{G}_{jk} - \mathcal{G}_{ik}\mathcal{G}_{jl}. \end{aligned} \tag{A2}$$

2. The Hubbard-Stratonovich transformation

It is well known that the coefficients γ_{ijlk} describing the interaction part of (1) satisfy the relation $\gamma^*_{ijlk} = \gamma_{lkij}$ and can be consequently cast in a hermitian matrix $\Gamma_{(ki)(jl)} = \gamma_{ijlk}$ of order M^2. Due to the spectral theorem $\Gamma_{(ki)(jl)} = \sum_{\zeta=1}^{M^2} \mathcal{U}^*_{\zeta(ki)}\ \Gamma_\zeta\ \mathcal{U}_{\zeta(jl)}$ for some real-valued coefficients Γ_ζ and some unitary matrix U of order M^2. As a consequence, (1) can be put in the form

$$\hat{H} = \hat{H}_0 - \frac{1}{2} \sum_{\zeta=1}^{M^2} \Gamma_\zeta \left[\frac{(\hat{O}_\zeta + \hat{O}^\dagger_\zeta)^2}{2} + \frac{(i\hat{O}_\zeta - i\hat{O}^\dagger_\zeta)^2}{2} \right], \tag{A3}$$

with

$$\begin{aligned} \hat{H}_0 &= \sum_{il} \left[\beta_{il} + \sum_j \gamma_{ijlj} \right] \hat{a}^\dagger_i \hat{a}_l, \\ \hat{O}_\zeta &= \sum_{jl} U_{\zeta(jl)}\ \hat{a}^\dagger_j \hat{a}_l. \end{aligned} \tag{A4}$$

Notice that the interaction part of (A4) has been replaced with a *sum of squares of single-particle hermitian operators*. Inserting such expression in $e^{-\delta\tau(\hat{H}-\epsilon_0)}$ and applying a Trotter-Suzuki decomposition:

$$e^{-\delta\tau(\hat{H}-\epsilon_0)} = e^{\delta\tau(\hat{H}_0-\epsilon_0)} \prod_{\zeta=1}^{M^2} e^{\frac{\delta\tau}{2}\Gamma_\zeta(\hat{O}_\zeta+\hat{O}^\dagger_\zeta)^2} e^{\frac{\delta\tau}{2}\Gamma_\zeta(i\hat{O}_\zeta - i\hat{O}^\dagger_\zeta)^2}. \tag{A5}$$

To each of the factors appearing in (A5) the Hubbard-Stratonovich Transformation applies, yielding (6) with

$$\hat{A}(\boldsymbol{\eta}) = \frac{\delta\tau}{2}(\hat{H}_0 - \epsilon_0) + \sum_\zeta \sqrt{\delta\tau\Gamma_\zeta}\,(\eta_{1,\zeta} + i\eta_{2,\zeta})\hat{O}_\zeta + h.c., \tag{A6}$$

which can be compactly written as

$$\hat{A}(\boldsymbol{\eta}) = \frac{\delta\tau}{2}(\hat{H}_0 - \epsilon_0) - \sqrt{\delta\tau}\, i\, \hat{\boldsymbol{B}} \cdot \boldsymbol{\eta}. \tag{A7}$$

3. The importance sampling transformation

We now explain in detail the derivation of Eq. (9). First we introduce in the expression (8) n arbitrary and possibly complex-valued shift parameters $\boldsymbol{\xi}_0 \dots \boldsymbol{\xi}_{n-1}$ obtaining

$$\begin{aligned} e^{-n\delta\tau(\hat{H}-\epsilon_0)}|\Psi_T\rangle \simeq \int & dg(\boldsymbol{\eta}_{n-1} - \boldsymbol{\xi}_{n-1}) \dots dg(\boldsymbol{\eta}_0 - \boldsymbol{\xi}_0) \\ & \times \hat{G}(\boldsymbol{\eta}_{n-1} - \boldsymbol{\xi}_{n-1}) \dots \hat{G}(\boldsymbol{\eta}_0 - \boldsymbol{\xi}_0)|\Psi_T\rangle. \end{aligned} \tag{A8}$$

Then we recall that

$$dg(\boldsymbol{\eta} - \boldsymbol{\xi}) = dg(\boldsymbol{\eta})\, e^{-\frac{\boldsymbol{\xi}\cdot\boldsymbol{\xi}}{2} - \boldsymbol{\eta}\cdot\boldsymbol{\xi}} \tag{A9}$$

and obtain (9) inserting the identity

$$\begin{aligned}
&\hat{G}(\boldsymbol{\eta}_{n-1}-\boldsymbol{\xi}_{n-1})\dots\hat{G}(\boldsymbol{\eta}_0-\boldsymbol{\xi}_0)|\Psi_T\rangle \\
&= \frac{\hat{G}(\boldsymbol{\eta}_{n-1}-\boldsymbol{\xi}_{n-1})\dots\hat{G}(\boldsymbol{\eta}_0-\boldsymbol{\xi}_0)|\Psi_T\rangle}{\langle\Psi_T|\hat{G}(\boldsymbol{\eta}_{n-1}-\boldsymbol{\xi}_{n-1})\dots\hat{G}(\boldsymbol{\eta}_0-\boldsymbol{\xi}_0)\Psi_T\rangle} \\
&\quad\times\prod_{k=0}^{n-1}\frac{\langle\Psi_T|\hat{G}(\boldsymbol{\eta}_k-\boldsymbol{\xi}_k)\dots\hat{G}(\boldsymbol{\eta}_0-\boldsymbol{\xi}_0)\Psi_T\rangle}{\langle\Psi_T|\hat{G}(\boldsymbol{\eta}_{k-1}-\boldsymbol{\xi}_{k-1})\dots\hat{G}(\boldsymbol{\eta}_0-\boldsymbol{\xi}_0)\Psi_T\rangle} \\
&\quad\times\frac{\langle\Psi_T|\hat{G}(\boldsymbol{\eta}_0-\boldsymbol{\xi}_0)\Psi_T\rangle}{\langle\Psi_T|\Psi_T\rangle} \\
&= \frac{\hat{G}(\boldsymbol{\eta}_{n-1}-\boldsymbol{\xi}_{n-1})\dots\hat{G}(\boldsymbol{\eta}_0-\boldsymbol{\xi}_0)|\Psi_T\rangle}{\langle\Psi_T|\hat{G}(\boldsymbol{\eta}_{n-1}-\boldsymbol{\xi}_{n-1})\dots\hat{G}(\boldsymbol{\eta}_0-\boldsymbol{\xi}_0)\Psi_T\rangle} \\
&\quad\times\mathfrak{W}[\boldsymbol{\eta}_{n-1},\boldsymbol{\xi}_{n-1}\dots\boldsymbol{\eta}_0,\boldsymbol{\xi}_0]. \qquad \text{(A10)}
\end{aligned}$$

So far, the shift parameters are arbitrary. We subsequently fix their values to contain fluctuations in the importance function and therefore in the weight function. To this purpose, we expand $\hat{G}(\boldsymbol{\eta}-\boldsymbol{\xi})$ up to $\sqrt{\delta\tau}$ obtaining

$$\hat{G}(\boldsymbol{\eta}-\boldsymbol{\xi}) = \mathbb{I} - i\sqrt{\delta\tau}\,(\boldsymbol{\eta}-\boldsymbol{\xi})\cdot\hat{\boldsymbol{B}} + \mathcal{O}(\delta\tau). \qquad \text{(A11)}$$

Introducing this approximation in (11) leads to

$$\begin{aligned}
\log[\mathfrak{I}[\boldsymbol{\eta},\boldsymbol{\xi};|\Psi\rangle]] &= -\frac{|\boldsymbol{\xi}|^2}{2} + \boldsymbol{\eta}\cdot\boldsymbol{\xi} - i\sqrt{\delta\tau}\,\frac{\langle\Psi_T|\boldsymbol{B}|\Psi\rangle}{\langle\Psi_T|\Psi\rangle} \\
&\quad\cdot(\boldsymbol{\eta}-\boldsymbol{\xi}), \qquad \text{(A12)}
\end{aligned}$$

where the operation $\frac{\langle\Psi_T|\cdot|\Psi\rangle}{\langle\Psi_T|\Psi\rangle}$ shall be henceforth abbreviated with $\langle\hat{\cdot}\rangle$. Imposing $\partial_{\boldsymbol{\eta}}\log[\mathfrak{I}[\boldsymbol{\eta},\boldsymbol{\xi};|\Psi\rangle]] = 0$ fixes the value of the shift parameters to

$$\boldsymbol{\xi}_{opt} = -i\sqrt{\delta\tau}\langle\hat{\boldsymbol{B}}\rangle. \qquad \text{(A13)}$$

Insertion of (A13) into (11) yields the stabilized expression for the importance function. A straightforward expansion of this quantity in powers of $\sqrt{\delta\tau}$ leads to

$$\begin{aligned}
\mathfrak{I}[\boldsymbol{\eta},\boldsymbol{\xi}_{opt};|\Psi\rangle] &= 1 - \delta\tau(\langle\hat{H}\rangle - \epsilon_0) \\
&\quad - \frac{\delta\tau}{2}[\langle|\boldsymbol{\eta}\cdot(\hat{\boldsymbol{B}}-\langle\hat{\boldsymbol{B}}\rangle)|^2\rangle - \langle|\hat{\boldsymbol{B}}-\langle\hat{\boldsymbol{B}}\rangle|^2\rangle] \\
&\quad + \mathcal{O}(\delta\tau^{3/2}). \qquad \text{(A14)}
\end{aligned}$$

The real local energy approximations (12) are suggested by the observation that the term in square brackets in (A14) has zero average over auxiliary field configurations, and it consists in neglecting all terms of order $\delta\tau$ in (A14) except for the real part of $\langle\hat{H}\rangle$. The imaginary part of $\langle\hat{H}\rangle$ is neglected because it vanishes for $|\Psi\rangle$ equal to the ground state. Empirical evidence shows that it is a reasonable approximation, but to our knowledge it is not supported by mathematical arguments.

4. The backpropagation technique

We now discuss the emergence of the backpropagated estimator (18). We express all imaginary time propagators appearing in (17) with (A8) and obtain the following representations for the numerator and the denominator:

$$\begin{aligned}
&\langle\Psi_T|e^{-(m+n)\delta\tau(\hat{H}-\epsilon_0)}|\Psi_T\rangle \\
&= \int dg(\boldsymbol{\eta}_{m+n-1})\dots dg(\boldsymbol{\eta}_0)\langle\Psi_T|\prod_{i=0}^{m+n-1}\hat{G}(\boldsymbol{\eta}_i)|\Psi_T\rangle, \qquad \text{(A15)} \\
&\langle\Psi_T|e^{-m\delta\tau(\hat{H}-\epsilon_0)}\hat{O}e^{-n\delta\tau(\hat{H}-\epsilon_0)}|\Psi_T\rangle \\
&= \int dg(\boldsymbol{\eta}_{m+n-1})\dots dg(\boldsymbol{\eta}_0)\langle\Psi_T| \\
&\quad\times\prod_{i=n}^{m+n-1}\hat{G}(\boldsymbol{\eta}_i)\hat{O}\prod_{i=0}^{n-1}\hat{G}(\boldsymbol{\eta}_i)|\Psi_T\rangle,
\end{aligned}$$

where the symbol $\prod_{i=i_1}^{i_2}\hat{G}(\boldsymbol{\eta}_i)$ stands for the product $\hat{G}(\boldsymbol{\eta}_{i_2})\dots\hat{G}(\boldsymbol{\eta}_{i_1})$. Further application of the importance sampling transformation and of identity (A10) yields

$$\begin{aligned}
&\langle\Psi_T|e^{-(m+n)\delta\tau(\hat{H}-\epsilon_0)}|\Psi_T\rangle \\
&= \int dg(\boldsymbol{\eta}_{m+n-1})\dots dg(\boldsymbol{\eta}_0)\mathfrak{W}[\boldsymbol{\eta}_{m+n-1},\boldsymbol{\xi}_{m+n-1}\dots\boldsymbol{\eta}_0,\boldsymbol{\xi}_0], \qquad \text{(A16)} \\
&\langle\Psi_T|e^{-m\delta\tau(\hat{H}-\epsilon_0)}\hat{O}e^{-n\delta\tau(\hat{H}-\epsilon_0)}|\Psi_T\rangle \\
&= \int dg(\boldsymbol{\eta}_{m+n-1})\dots dg(\boldsymbol{\eta}_0)\mathfrak{W}[\boldsymbol{\eta}_{m+n-1},\boldsymbol{\xi}_{m+n-1}\dots\boldsymbol{\eta}_0,\boldsymbol{\xi}_0] \\
&\quad\times\frac{\langle\Psi_T|\prod_{i=n}^{m+n-1}\hat{G}(\boldsymbol{\eta}_i-\boldsymbol{\xi}_i)\hat{O}\prod_{i=0}^{n-1}\hat{G}(\boldsymbol{\eta}_i-\boldsymbol{\xi}_i)|\Psi_T\rangle}{\langle\Psi_T|\prod_{i=0}^{m+n-1}\hat{G}(\boldsymbol{\eta}_i-\boldsymbol{\xi}_i)|\Psi_T\rangle}
\end{aligned}$$

the estimator for which is obviously (18). Notice that *the same weights appearing in* (15) are involved in (18).

5. The phaseless AFQMC estimator for ITCFs

We now explain in detail the derivation of Eqs. (22) and (23). The last passage of (22) is a manipulation of the operator product $\hat{G}(\boldsymbol{\eta}_{n-1})\dots\hat{G}(\boldsymbol{\eta}_{n-r})\hat{a}_k^\dagger\hat{a}_l$. First, we observe that if $\hat{A} = \sum_{i,j}\mathcal{A}_{i,j}\hat{a}_i^\dagger\hat{a}_j$ is a one-body operator:

$$\begin{aligned}
e^{\tau\hat{A}}\hat{a}_k^\dagger e^{-\tau\hat{A}} &= \sum_i[e^{\tau\mathcal{A}}]_{ik}\hat{a}_i^\dagger, \\
e^{\tau\hat{A}}\hat{a}_l e^{-\tau\hat{A}} &= \sum_j[e^{-\tau\mathcal{A}}]_{lj}\hat{a}_j.
\end{aligned} \qquad \text{(A17)}$$

As an immediate consequence:

$$e^{\tau\hat{A}}\hat{a}_k^\dagger\hat{a}_l = \sum_{ij}[e^{\tau\mathcal{A}}]_{ik}\hat{a}_i^\dagger\hat{a}_j[e^{-\tau\mathcal{A}}]_{lj}\,e^{\tau\hat{A}} \qquad \text{(A18)}$$

showing that the exponential of a one-body operator can be moved to the right of a product $\hat{a}_k^\dagger\hat{a}_l$ at the cost of introducing the matrix $e^{\tau\mathcal{A}}$ and its inverse. Iterated application of formula (A18) to the operator product $\hat{G}(\boldsymbol{\eta}_{n-1})\dots\hat{G}(\boldsymbol{\eta}_{n-r})\hat{a}_k^\dagger\hat{a}_l$ yields

$$\begin{aligned}
&\hat{G}(\boldsymbol{\eta}_{n-1})\dots\hat{G}(\boldsymbol{\eta}_{n-r})\hat{a}_k^\dagger\hat{a}_l \\
&= \sum_{ij}[e^{\mathcal{A}(\boldsymbol{\eta}_{n-r})}\dots e^{\mathcal{A}(\boldsymbol{\eta}_{n-1})}]_{ik}[e^{-\mathcal{A}(\boldsymbol{\eta}_{n-1})}\dots e^{-\mathcal{A}(\boldsymbol{\eta}_{n-r})}]_{lj} \\
&\quad\times\hat{a}_i^\dagger\hat{a}_j\hat{G}(\boldsymbol{\eta}_{n-1})\dots\hat{G}(\boldsymbol{\eta}_{n-r}) \qquad \text{(A19)}
\end{aligned}$$

and justifies the last passage of Eq. (22). To obtain (23) we observe, as in the backpropagation technique, that

$$F_{\hat{A},\hat{B}}(r\delta\tau) \simeq \frac{1}{N}\frac{1}{\langle\Psi_T|e^{-(m+n-r)\delta\tau(\hat{H}-\epsilon_0)}|\Psi_T\rangle} \cdot \langle\Psi_T|e^{-m\delta\tau(\hat{H}-\epsilon_0)}\hat{A}e^{-r\delta\tau(\hat{H}-\epsilon_0)} \times \hat{B}e^{-(n-r)\delta\tau(\hat{H}-\epsilon_0)}|\Psi_T\rangle; \tag{A20}$$

notice that, unlike in (17), at the denominator of the previous equation only $m+n-r$ integrations over auxiliary fields configurations are involved. Expressing all imaginary time propagators appearing in (A20) with (A8), recalling (22), and applying the importance sampling transformation to both numerator and denominator of the previous equation lead to

$$\begin{aligned}&\langle\Psi_T|e^{-(m+n-r)\delta\tau(\hat{H}-\epsilon_0)}|\Psi_T\rangle \\ &= \int dg(\boldsymbol{\eta}_{m+n-1})\dots dg(\boldsymbol{\eta}_n)dg(\boldsymbol{\eta}_{n-r})\dots dg(\boldsymbol{\eta}_0) \\ &\quad\times\langle\Psi_T|\prod_{i=n}^{m+n-1}\hat{G}(\boldsymbol{\eta}_i)\prod_{i=0}^{n-r-1}\hat{G}(\boldsymbol{\eta}_i)|\Psi_T\rangle,\end{aligned} \tag{A21}$$

$$\begin{aligned}&\langle\Psi_T|e^{-m\delta\tau(\hat{H}-\epsilon_0)}\hat{A}e^{-r\delta\tau(\hat{H}-\epsilon_0)}\hat{B}e^{-n\delta\tau(\hat{H}-\epsilon_0)}|\Psi_T\rangle \\ &= \sum_{ijkl}\mathcal{B}_{kl}\int dg(\boldsymbol{\eta}_{m+n-1})\dots dg(\boldsymbol{\eta}_0) \\ &\quad\times\langle\Psi_T|\prod_{i=n}^{m+n-1}\hat{G}(\boldsymbol{\eta}_i)\hat{A}\hat{a}_i^\dagger\hat{a}_j\prod_{i=0}^{n-1}\hat{G}(\boldsymbol{\eta}_i)|\Psi_T\rangle \\ &\quad\times\mathcal{D}(\boldsymbol{\eta}_{n-1}\dots\boldsymbol{\eta}_{n-r})_{ik}\mathcal{D}^{-1}(\boldsymbol{\eta}_{n-1}\dots\boldsymbol{\eta}_{n-r})_{lj}.\end{aligned} \tag{A22}$$

Further application of the importance sampling transformation and of identity (A10) yields

$$\begin{aligned}&\langle\Psi_T|e^{-(m+n-r)\delta\tau(\hat{H}-\epsilon_0)}|\Psi_T\rangle \\ &= \int dg(\boldsymbol{\eta}_{m+n-1})\dots dg(\boldsymbol{\eta}_n)dg(\boldsymbol{\eta}_{n-r})\dots dg(\boldsymbol{\eta}_0) \\ &\quad\times\langle\Psi_T|e^{-m\delta\tau(\hat{H}-\epsilon_0)}\hat{A}e^{-r\delta\tau(\hat{H}-\epsilon_0)}\hat{B}e^{-n\delta\tau(\hat{H}-\epsilon_0)}|\Psi_T\rangle \\ &= \mathfrak{W}[\boldsymbol{\eta}_{m+n-1},\boldsymbol{\xi}_{m+n-1}\dots\boldsymbol{\eta}_n,\boldsymbol{\xi}_n\boldsymbol{\eta}_{n-r},\boldsymbol{\xi}_{n-r}\dots\boldsymbol{\eta}_0,\boldsymbol{\xi}_0] \\ &\quad\times\langle\Psi_T|e^{-m\delta\tau(\hat{H}-\epsilon_0)}\hat{A}e^{-r\delta\tau(\hat{H}-\epsilon_0)}\hat{B}e^{-n\delta\tau(\hat{H}-\epsilon_0)}|\Psi_T\rangle\end{aligned} \tag{A23}$$

expanding the propagators involved in (A23) we find

$$\begin{aligned}&\langle\Psi_T|e^{-(m+n-r)\delta\tau(\hat{H}-\epsilon_0)}|\Psi_T\rangle \\ &= \sum_{ijkl}\mathcal{B}_{kl}\int dg(\boldsymbol{\eta}_{m+n-1})\dots dg(\boldsymbol{\eta}_0) \\ &\quad\times\mathfrak{W}[\boldsymbol{\eta}_{m+n-1},\boldsymbol{\xi}_{m+n-1}\dots\boldsymbol{\eta}_0,\boldsymbol{\xi}_0] \\ &\quad\times\frac{\langle\Psi_T|\prod_{i=n}^{m+n-1}\hat{G}(\boldsymbol{\eta}_i-\boldsymbol{\xi}_i)\hat{A}\hat{a}_i^\dagger\hat{a}_j\prod_{i=0}^{n-1}\hat{G}(\boldsymbol{\eta}_i-\boldsymbol{\xi}_i)|\Psi_T\rangle}{\langle\Psi_T|\prod_{i=0}^{m+n-1}\hat{G}(\boldsymbol{\eta}_i-\boldsymbol{\xi}_i)|\Psi_T\rangle} \\ &\quad\times\mathcal{D}(\boldsymbol{\eta}_{n-1}-\boldsymbol{\xi}_{n-1}\dots\boldsymbol{\eta}_{n-r}-\boldsymbol{\xi}_{n-r})_{ik} \\ &\quad\times\mathcal{D}^{-1}(\boldsymbol{\eta}_{n-1}-\boldsymbol{\xi}_{n-1}\dots\boldsymbol{\eta}_{n-r}-\boldsymbol{\xi}_{n-r})_{lj}\end{aligned} \tag{A24}$$

an estimator for which is precisely (23). Notice that the numerator (A24) of the estimator (A20) involves an integration over $n+m$ auxiliary fields configurations, whereas the denominator (A23) involves an integration over $n+m-r$ auxiliary fields configurations. Due to this circumstance, the weights $\mathfrak{W}_{m+n}^{(w)}$ appearing in the numerator of (23) coincide with those appearing in (18), whereas at the denominator *other weights* $\mathfrak{W}_{m+n-r}^{(w)}$ *appear*, which are constructed with a slightly modified recursion relation:

$$\mathfrak{W}_{k+1}^{(w)} = \begin{cases}\mathfrak{W}_k^{(w)} & \text{if } n-r\le k\le n-1 \\ \mathfrak{W}_k^{(w)}\,\mathfrak{I}\left[\boldsymbol{\eta}_k^{(w)},\boldsymbol{\xi}_k^{(w)};|\Psi_k^{(w)}\rangle\right] & \text{otherwise}\end{cases}. \tag{A25}$$

APPENDIX B: ITCFs FOR THE IDEAL FERMI GAS

In the case of a noninteracting system, the ITCF $F_{\mathbf{q}}(\tau)$ takes the form

$$\begin{aligned}F_{\mathbf{q}}(\tau) &= \frac{1}{N}\langle\Psi_0|\hat{\rho}_{\boldsymbol{q}}(\tau)\hat{\rho}_{-\boldsymbol{q}}|\Psi_0\rangle \\ &= \frac{1}{N}\sum_{\boldsymbol{p},\boldsymbol{p}'}\sum_{\sigma\sigma'}\langle\Psi_0|\hat{a}^\dagger_{\boldsymbol{p}-\boldsymbol{q},\sigma}(\tau)\hat{a}_{\boldsymbol{p},\sigma}(\tau)\hat{a}^\dagger_{\boldsymbol{p}'+\boldsymbol{q},\sigma'}\hat{a}_{\boldsymbol{p}',\sigma'}|\Psi_0\rangle.\end{aligned} \tag{B1}$$

For a spin polarized system, using Heisenberg representation and Wick's theorem, formula (B1) can be reduced to

$$F_{\mathbf{q}}(\tau) = \frac{1}{N}\sum_{\boldsymbol{p}}e^{-\tau(\epsilon_p-\epsilon_{p-q})}\,\Theta(k_F-|\boldsymbol{p}-\boldsymbol{q}|)\,\Theta(|\boldsymbol{p}|-k_F). \tag{B2}$$

Numeric evaluation of (B2) yields $F_{\mathbf{q}}(\tau)$. For $N_\uparrow = 5$, $N_\downarrow = 0$, $r_s = 1$, and $\boldsymbol{q} = \frac{2\pi}{L}(1,0)$ the nonvanishing contributions to (B2) come from $\boldsymbol{p} = \frac{2\pi}{L}(1,0)$, $\frac{2\pi}{L}(0,1)$, $\frac{2\pi}{L}(0,-1)$. Consequently,

$$F_{\mathbf{q}}(\tau) = \frac{e^{-\frac{6\pi}{5}\tau}}{5} + \frac{2e^{-\frac{2\pi}{5}\tau}}{5}. \tag{B3}$$

[1] M. H. Kalos, Phys. Rev. **128**, 1791 (1962).
[2] M. Boninsegni and D. M. Ceperley, J. Low Temp. Phys. **104**, 339 (1996).
[3] S. Baroni and S. Moroni, Phys. Rev. Lett. **82**, 4745 (1999).
[4] A. Sarsa, K. E. Schmidt, and W. Magro, J. Chem. Phys. **113**, 1366 (2000).
[5] D. E. Galli and L. Reatto, Mol. Phys. **101**, 1697 (2003).
[6] M. Rossi, M. Nava, L. Reatto, and D. E. Galli, J. Chem. Phys. **131**, 154108 (2009).
[7] M. Jarrell and J. E. Gubernatis, Phys. Rep. **269**, 133 (1996).
[8] S. R. White, *Computer Simulation Studies in Condensed Matter Physics III* (Springer Verlag, 1991).
[9] O. F. Syljuåsen, Phys. Rev. B **78**, 174429 (2008).
[10] D. R. Reichman and E. Rabani, J. Chem. Phys. **131**, 054502 (2009).
[11] A. W. Sandvik, Phys. Rev. B **57**, 10287 (1998).
[12] E. Vitali, M. Rossi, L. Reatto, and D. E. Galli, Phys. Rev. B **82**, 174510 (2010).
[13] M. Rossi, E. Vitali, L. Reatto, and D. E. Galli, Phys. Rev. B **85**, 014525 (2012).
[14] R. P. Feynman and A. R. Hibbs, *Quantum Mechanics and Path Integrals* (McGraw-Hill, 1965).
[15] E. Y. Loh *et al.*, Phys. Rev. B **41**, 9301 (1990).
[16] J. Anderson, J. Chem. Phys. **63**, 1499 (1975).
[17] P. J. Reynolds, D. M. Ceperley, B. J. Alder, and W. A. Lester, J. Chem. Phys. **77**, 5593 (1982).

[18]G. H. Booth, A. J. W. Thom, and A. Alavi, J. Chem. Phys. **131**, 054106 (2009).
[19]M. Nava, A. Motta, D. E. Galli, E. Vitali, and S. Moroni, Phys. Rev. B **85**, 184401 (2012).
[20]R. Blankenbecler, D. J. Scalapino, and R. L. Sugar, Phys. Rev. D **24**, 2278 (1981).
[21]G. Sugiyama and S. E. Koonin, Ann. Phys. **168**, 1 (1986).
[22]S. Zhang and H. Krakauer, Phys. Rev. Lett. **90**, 136401 (2003).
[23]S. Zhang, H. Krakauer, W. A. Al Saidi, and M. Suewettana, Comput. Phys. Commun. **169**, 394 (2005).
[24]M. Feldbacher and F. F. Assaad, Phys. Rev. B **63**, 073105 (2001).
[25]G. Booth and G. Chan, J. Chem. Phys. **137**, 191102 (2012).
[26]S. Zhang, *Theoretical Methods for Strongly Correlated Electron Systems* (Springer Verlag, 2003).
[27]W. Purwanto and S. Zhang, Phys. Rev. E **70**, 056702 (2004).
[28]W. Purwanto, S. Zhang, and H. Krakauer, J. Chem. Phys. **130**, 094107 (2009).
[29]W. Purwanto, H. Krakauer, Y. Virgus, and S. Zhang, J. Chem. Phys. **135**, 164105 (2011).
[30]W. Purwanto, H. Krakauer, and S. Zhang, Phys. Rev. B **80**, 214116 (2009).
[31]K. P. Esler *et al.*, J. Phys.: Conf. Ser. **125**, 012057 (2008).
[32]H. F. Trotter, Proc. Am. Math. Soc. **10**, 545 (1959).
[33]M. Suzuki, Prog. Theor. Phys. **56**, 1454 (1976).
[34]J. Hubbard, Phys. Rev. Lett. **3**, 77 (1959).
[35]R. L. Stratonovich, Sov. Phys. Dokl. **2**, 416 (1957).
[36]C. J. Umrigar, M. P. Nightingale, and K. J. Runge, J. Chem. Phys. **99**, 2865 (1993).
[37]P. P. Ewald, Ann. Phys. **369**, 253 (1921).
[38]W. Givens, Oak Ridge Report Number ORNL 1574 (1954).
[39]L. S. Blackford, J. Choi *et al.*, *ScaLAPACK Users' Guide* (Society for Industrial and Applied Mathematics, 1997).
[40]E. Y. Loh and J. E. Gubernatis, *Electronic Phase Transitions* (North-Holland, Amsterdam, 1992).
[41]Y. Kwon, D. M. Ceperley, and R. M. Martin, Phys. Rev. B **53**, 7376 (1996).
[42]C. N. Gilbreth and Y. Alhassid, e-print arXiv:1210.4131 (2013).
[43]D. J. Thouless, Nucl. Phys. **21**, 225 (1960).
[44]R. Balian and E. Brezin, Nuovo Cimento B **64**, 37 (1969).